Synthesis of Mesoporous Silica from Sugarcane Bagasse Ash Using Pluronic 123 as a Colorant Adsorbent for Brilliant Green

Sukirna, Iwan
Department of Metallurgical and Materials Engineering, University of Indonesia

Dhaneswara, Donanta
Department of Metallurgical and Materials Engineering, University of Indonesia

Davina Jennifa Siregar
Department of Metallurgical and Materials Engineering, University of Indonesia

Jaka Fajar Fatriansyah
Department of Metallurgical and Materials Engineering, University of Indonesia

他

https://doi.org/10.5109/7183448

出版情報：Evergreen. 11 (2), pp.1366-1374, 2024-06. 九州大学グリーンテクノロジー研究教育センター
バージョン：

Synthesis of Mesoporous Silica from Sugarcane Bagasse Ash Using Pluronic 123 as a Colorant Adsorbent for Brilliant Green

Iwan Sukirna[1,*], Donanta Dhaneswara[1,*], Davina Jennifa Siregar[1], Jaka Fajar Fatriansyah[1], Nofrijon Sofyan[1], Akhmad Herman Yuwono[1], Rifai Muslih[2]

[1]Department of Metallurgical and Materials Engineering, University of Indonesia, Indonesia

[2]National Research and Innovation Agency (BRIN), Indonesia

E-mail: donanta.dhaneswara@ui.ac.id (D. Dhaneswara)
iwan.sukirna@ui.ac.id (I. Sukirna)

(Received October 24, 2023; Revised January 30, 2024; Accepted March 5, 2024).

Abstract: Mesoporous silica exhibits excellent adsorption capabilities, making it suitable for the treatment of colorant dye waste. However, the commonly used silica precursors, such as tetraethyl orthosilicate (TEOS) and tetramethyl orthosilicate (TMOS) are relatively expensive. Therefore, it prompts the exploration of biomass as an alternative precursor for mesoporous silica due to its affordability and widespread availability. Previous research has demonstrated the potential of rice husk and corn cob biomass can serve as alternative raw materials for mesoporous silica due to their high silica content. In this study, mesoporous silica was synthesized using sugar cane bagasse ash (SCBA) as the precursor, as it contains silica content ranging from 50-70% following combustion. The synthesis was performed using the Pluronic 123 surfactant template through the sol-gel method. The cationic dye brilliant green was used as the adsorbate in this research. Characterization techniques employed included Fourier-transform infrared spectroscopy (FTIR), scanning electron spectroscopy (SEM), Brunauer-Emmett-Teller (BET), small angle x-ray scattering (SAXS), and UV-Visible analysis. The resulting mesoporous silica exhibited surface area, pore radius, and pore volume of 363.4 m^2/g, 1.5434 nm, and 0.716 cc/g, respectively, as well as 55.1% of cationic dye adsorption capacity. The present study demonstrated that the fabrication of mesoporous silica using sugarcane bagasse ash as the silica precursor has potential as an effective and economical adsorbent for industrial applications.

Keywords: sugarcane bagasse, surfactant, sol-gel method, mesoporous silica, dye adsorption

1. Introduction

Indonesia is an agricultural country, as most of its population works in the agricultural sector. One abundant agricultural product in Indonesia is sugarcane. Central Bureau of Statistics (BPS) stated that, in 2020, the total area of sugarcane plantations in Indonesia was 432.93 thousand hectares, which increased to 443.51 thousand hectares in 2021. This increase is also accompanied by a rise in sugarcane production in Indonesia, reaching 2.42 million tons in 2021, 2.13 million tons in 2020, and 2.23 million tons in 2019. The escalation in sugar production unavoidably entails a commensurate surge in sugarcane residue, leading to potential environmental concerns unless appropriately harnessed and managed[1)].

Bagasse is a byproduct of the sugar production process. Approximately 35-40% of the total weight of sugarcane subjected to milling comprises bagasse. Typically, 60% of the bagasse is utilized as fuel in sugar mills, as raw material for compost production, and as animal feed, leaving around 40% of bagasse underutilized[2–4)]. Therefore, alternative methods need to be considered for the effective utilization of bagasse, such as employing it as an adsorbent for colorants in textile wastewater through mesoporous silica[5)].

Mesoporous materials are characterized by pores with diameters ranging from 2 to 50 nm. One commonly used compound for mesoporous materials is SiO_2 (silica) due to its numerous advantages, such as excellent stability, inertness, biocompatibility, and compatibility with the human body[6–8)]. The first synthesis of mesoporous silica was achieved in 1992 by the Mobil Corporation and was

named Mobil Crystalline of Material (MCM-41). This discovery triggered a surge of interest among researchers to further explore the field of mesoporous materials[9]. In 1988, researchers from the University of California Santa Barbara discovered another mesoporous material with similar characteristics to MCM-41, featuring uniform hexagonal-shaped pores but with larger pore diameters. This material was named Santa Barbara Amorphous-15 (SBA-15)[10]. Typically, the synthesis of SBA-15 to achieve the desired pore diameter involves the use of the surfactant Pluronic 123[11]. SBA-15 is a mesoporous silica material where the source of silica is derived from chemical compounds such as Tetraethyl Orthosilicate (TEOS), Tetramethyl Orthosilicate (TMOS), or Tetraprophyl Orthosilicate (TPOS), which are relatively expensive[12].

Therefore, there is a need to explore alternative, more affordable sources of silica that are readily available. Agricultural waste is one of the alternative silica source solutions that are now attracting the attention of researchers to create inexpensive silica-based adsorbents with performance that is competitive with synthetic silica sources. Thu et al. (2019) successfully synthesized mesoporous silica from rice husk ash that has 91.9% removal of methylene blue after 50 minutes of adsorption[13]. On the other hand, Dhaneswara et al. (2022) achieved removal percentages of 77.05% and 74.08% for 10 mg/L methylene blue using mesoporous silica from rice husk and corn cob ash[14]. Hence, in this study, mesoporous silica will be synthesized from agricultural waste, specifically sugarcane bagasse, as the silica source in an effort of waste utilization to address environmental waste issues. By subjecting sugarcane bagasse to combustion, sugarcane bagasse ash (SCBA) can be obtained, which has a high silica (SiO_2) content ranging from 50-70%[13]. This ash holds potential to be used for the synthesis of mesoporous silica. Mesoporous silica can be applied to many applications, such as in textile industry, drug delivery systems, energy application, catalysis, and many more because of its unique porous structure and high surface area[14].

The textile industry remains one of the largest industries in Indonesia, which is why textile waste continues to be a major source of water pollution. The wastewater from textile processes mainly consists of residual dyes, with a significant portion being azo dyes such as brilliant green. This dye is carcinogenic due to the presence of hazardous aromatic groups that pose risks to living organisms' health. Therefore, efforts need to be made to minimize the levels of this dye before discharging textile wastewater into water bodies or reusing it for production. One approach to address this issue is through adsorption using mesoporous silica. This study aims to investigate the adsorption process of brilliant green by the synthesized mesoporous silica with varying adsorption times.

2. Materials and Methods

2.1 Materials

The raw material used in this study was sugarcane bagasse ash (SCBA) obtained from Blitar, East Java. The other material used was sodium hydroxide (NaOH) (Supelco), which serves to bind the silica from the SCBA. The equipments used for the synthesis of the silica precursor from sugarcane bagasse included beaker glass, filter paper, magnetic stirrer, Erlenmeyer flask, glass funnel, condenser, static, and clamp. For the preparation of the surfactant solution, the materials used included Pluronic 123 (Sigma-Aldrich) and a 1.6 M hydrochloric acid (HCl) (Supelco) solution, with a total volume of 380 ml. The equipment used for this process included beaker glass, graduated cylinder, magnetic stirrer, and analytical balance. The materials used in the synthesis of mesoporous silica included Na_2SiO_3 filtrate and Pluronic 123 surfactant. Aquadest (deionized water) was also used for washing the formed gel. The equipment utilized in this process included beaker glass, magnetic stirrer, pipette, graduated cylinder, filter paper, glass funnel, oven, spatula, and Erlenmeyer flask. The drying process was carried out using an oven, while the calcination process was performed using a furnace, crucible, and glass wool. The dye adsorption testing was then conducted by preparing 10 ppm solutions of brilliant green by dissolving 10 mg of brilliant green powder with aquadest until 1 liter. The equipment used for this process included beaker glass, graduated cylinder, magnetic stirrer, glass funnel, stopwatch, pipette, stirring rod, and cuvette.

2.2 Synthesis Mesoporous Silica

The primary raw material for this research was sugarcane bagasse obtained from natural resource waste, which was subsequently incinerated to obtain sugarcane bagasse ash. The initial step in this process involved washing the sugarcane bagasse with water, followed by sun-drying for 8 hours to reduce the moisture content in the bagasse. Subsequently, the sugarcane bagasse underwent incineration at 700ºC for 6 hours in order to reduce impurities and acquire white-colored SCBA.

The production of silica precursor involved adding 12.5 grams of SCBA to a 10% w/v NaOH solution, followed by incubation for 24 hours and refluxing for 1 hour at 80ºC. The final outcome of this process was a precursor of silica in the form of sodium silicate (Na_2SiO_3) with a yellowish color according to reaction Equation (1) [15].

The sol-gel preparation process began by creating a Pluronic 123 surfactant solution. Pluronic 123 is an amphipathic triblock copolymer, where the hydrophilic and hydrophobic blocks are poly(ethylene oxide) (POE) and poly(propylene oxide) (PPO), respectively, with a structure of PEO20-PPO70-PEO20 that acts as a directing agent[16]. This process involved mixing 15 grams of Pluronic 123 with a 1.6 M HCl solution containing 380 ml, utilizing a magnetic stirrer for thorough mixing. The HCl

solution was prepared by diluting 37% HCl with aquadest until it reached a concentration of 1.6 M. Once the surfactant was dissolved in the HCl solution, the silica precursor was added drop by drop to the surfactant solution, with a total volume of 200 ml, while continuously stirred with a magnetic stirrer for 10 minutes according to Equation (2). Subsequently, the resulting mixture was transferred to an oven and subjected to aging at 40ºC for 24 hours [17]. The outcome of the aging process was the formation of a white precipitate, representing the sol-gel, which was then filtered to collect the precipitate [18,19]. The condensation process involved the addition of an acid, which hydrated the hydroxyl groups (-OH) of silanols (Si-OH), resulting in the protonation of the silicon atom in the silanol group, forming silicone ions (Si^+). The formation of Si^+ ions lead to the attack of oxygen atoms from other silanol groups, resulting in Equation (3) and the generation of siloxane bridges (Si-O-Si), accompanied by the release of H^+ ions[20].

$$SiO_2 + 2NaOH \rightarrow Na_2SiO_3 + H_2O \quad (1)$$

$$Na_2SiO_3 + xH_2O + 2H^- \rightarrow SiO_2(x+1)H_2O + 2Na^+ (2)$$

$$Si - OH + Si^+ \rightarrow Si - O - Si + H^+(x) \quad (3)$$

After the gel precipitate was filtered, it was dried for 24 hours at 100ºC in an oven. Once dried, the precipitate was washed with aquadest and subjected to a second drying process for 8 hours at the same temperature as the initial drying stage. Following this, the dried product was cooled to room temperature.

Calcination was carried out with the aim of removing Pluronic 123 surfactant as the template from the desired mesoporous structure [21]. The procedure was carried out by introducing silica powder into an oxygen-free furnace using a crucible and sealing it with glass wool. Heating was performed for 6 hours at 500ºC, resulting in mesoporous silica powder. This step marked the final stage of mesoporous silica synthesis, followed by characterization using SAXS (Shimadzu XRD-7000 at 2θ angles in the range of 0°-5° using CuKα with 1.54 Å wavelength), SEM (Field emission-SEM FEI Inspect F50), BET, and FTIR (TwoTM infrared spectrometer, PerkinElmer ASTM E 1252) testing to determine the formed surface and pores characteristics[22].

The formed mesoporous silica powder was then subjected to adsorption testing with brilliant green. A 10-ppm dye solution was prepared in a 50 ml beaker glass and stirred using a magnetic stirrer. Next, 50 mg of mesoporous silica powder was added to the solution and stirred for 3 hours using a magnetic stirrer. Using a pipette, 7 ml of the solution was taken every hour and put into a cuvette for UV-Vis analysis. The adsorption spectra resulted from UV-Vis could be used to calculate the adsorption capacity (qt) and the removal percentage of brilliant green dye (% removal) according to Equation (4) and Equation (5).

$$\boldsymbol{qt} = \frac{(\boldsymbol{C_o} - \boldsymbol{C_t})\,\boldsymbol{V}}{\boldsymbol{m}} \quad (4)$$

$$\%\boldsymbol{Removal} = \frac{(\boldsymbol{C_o} - \boldsymbol{C_t})}{\boldsymbol{Co}} \quad (5)$$

3. Result and Discussion

3.1 Identification of Functional Groups

Functional group identification on the synthesized mesoporous silica was performed using Fourier Transformed Infra-Red Spectroscopy (FTIR) characterization. The FTIR analysis results provided a graph displaying wavelengths that correspond to the specific functional group contained. From the FTIR graph of the sample (Fig. 1), various wavelengths indicate the formation of specific bonds in the mesoporous silica.

The FTIR analysis results revealed that the peaks observed at specific wavelengths corresponded to O-H, H-O-H, and Si-O-Si functional groups. On the other hand, different intensities in the FTIR spectrum were generated for different concentration of functional groups contained in mesoporous silica, where lower transmission intensity at a specific peak wavelength indicated a higher concentration of functional groups in the mesoporous silica.

The bond types identified in the synthesized mesoporous silica and their intensities are presented in Table 1. At a wavelength of 3380 cm^{-1}, the weak and broad transmission indicates the O-H stretching vibrations[23]. The magnitude of transmission indicates the quantity of O-H functional groups present in the mesoporous silica powder. These groups are the result of Si-OH bond formation and water molecules that were absorbed[24]. H-O-H vibrations indicating structure of water were also observed at a wavelength of 1631 cm^{-1} [25]. Additionally, the siloxane bridges (Si-O-Si) can be observed at the wavenumber of 3380, 793, and 452 cm^{-1}, indicating the asymmetric, symmetric, and torsional Si-O-Si, respectively.

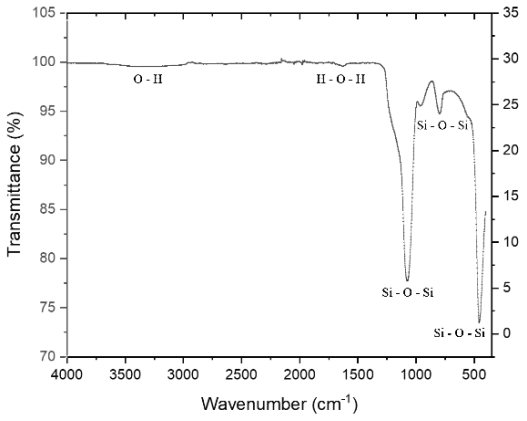

Fig. 1: FTIR spectrum of SCBA-based mesoporous silica

Table 1. The types of bonds in SCBA-based mesoporous silica

Functional Groups	Wavenumber (cm^{-1})	Transmittance (%)
O-H	3380	99.4
H-OH	1631	99.5
Si-O-Si (asymmetry)	1073	77.7
Si-O-Si (symmetry)	793	94.6
Si-O-Si (torque)	452	73.6

3.2 Chemical Composition and Surface Morphology

Micrographs of the SCBA-based mesoporous silica sample produced with Pluronic 123 are shown in Fig. 2. The process of enlargement was conducted at magnifications of 5000 and 10.000 times. From the pictures, it can be seen that the morphology of particles adopts a chain-like structure that defines coarse aggregates with a slight presence of spherical forms. The hydrophobic tails of Pluronic 123 hinder the connection between the silicate matrix and water, leading to a reduction in the speed of hydrolysis and an improvement in the stability of silicate while it solidifies. When surfactant concentration is added to an aqueous solution, the surfactant molecules accumulate at the surface, leading to a decrease in surface tension. If the surfactant concentration continues to increase, the surface tension will decrease linearly until it reaches the critical micelle concentration (CMC)[26]. At this point, the surface tension has reached its minimum value, even if more surfactant is added. It is at this condition that micelle aggregates start to form. However, it leads to a higher likelihood of nucleation events rather than particle growth. Consequently, this promotes the formation of smaller particles. The production of these particles could be ascribed to errors in weighing the Pluronic 123 surfactant, which led to an excess of surfactant beyond the desired optimum amount[27]

The EDS analysis for selected SCBA is presented in Fig. 3 and Table 2. The EDS characterization findings validate that the samples primarily consisted of silicon and oxygen atoms, indicating a high level of purity in the produced silica. Some impurities were detected in SCBA, which is to be expected in natural sources. The presence of sodium can be attributed to the incomplete hydrolysis process that occurs during the ion exchange of Na^+ with H^+ to form silanol (Si-OH) groups. In order to thoroughly remove impurities, it is imperative to ensure the flawless execution of all processes and carry out acid washing.

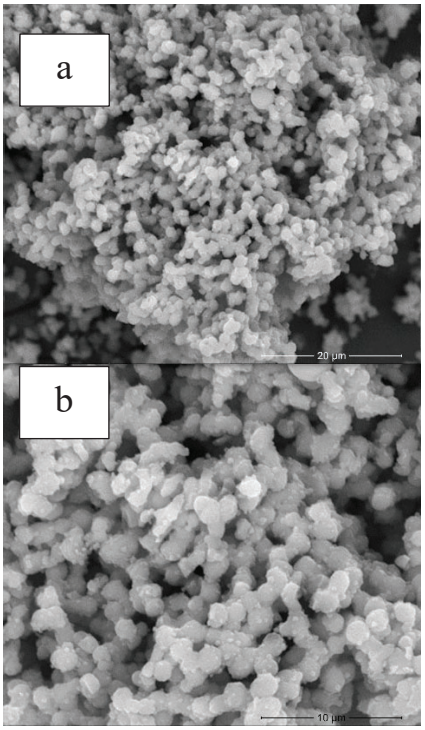

Fig. 2: SEM Images for SCBA Mesoporous (a) 5000x Magnification; (b) 10.000x Magnification

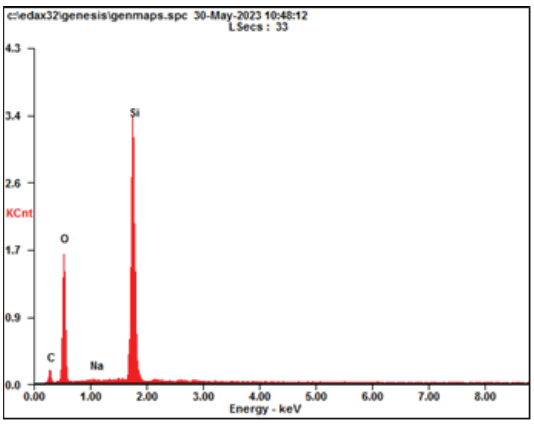

Fig. 3:. EDS analysis results of SCBA-based mesoporous silica

Table 2. EDS analysis table of SCBA-based mesoporous silica

Element	Line	Weight (%)	Atomic (%)
C	K	9,31	14,56
O	K	48,95	57,46
Si	K	41,29	27,61
Na	K	0,45	0,37

3.3 Isothermal Adsorption-Desorption Curve

The mesoporous silica was characterized using the Brunauer-Emmet-Teller (BET) nitrogen gas adsorption-desorption test to investigate pore characteristics, which consist of surface area, pore diameter, and pore volume[28].

The adsorption-desorption curve obtained from the BET analysis is presented in Fig. 4. According to IUPAC, the adsorption-desorption isotherm curves are classified into six types[29]. From Fig. 4, the adsorption-desorption curve of mesoporous silica synthesized from SCBA and

Pluronic 123 falls into type IV. The characteristic indication that the curve belongs to type IV is the presence of a hysteresis loop. The curvature at relative pressures between roughly 0.5 and 0.95 P/Po indicates the presence of capillary condensation within the mesoporous silica during the adsorption process, which is what causes the hysteresis loop[30]. This indicated that the sample in this study is a mesoporous material. The shape of the hysteresis loop observed in the graph corresponds to type H3, which indicates the presence of wedge-shaped pores. This behavior is attributed to the relatively low curvature of the pores and the lack of rigidity in the aggregate structure. Additionally, the shape of the H3 loop is influenced by the flexible nature of the adsorbent and the distinctive shoulder position indicates the destabilization of the condensed phase when the P/Po value reaches its limit[31].

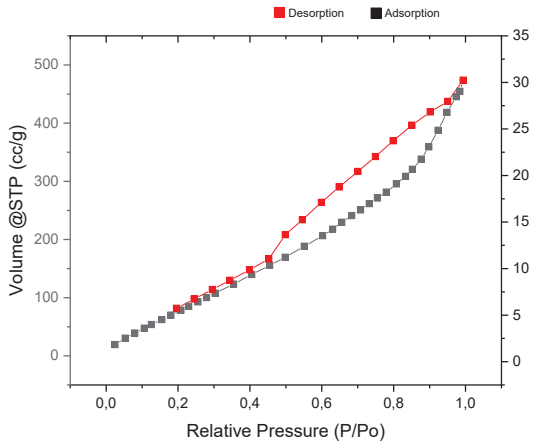

Fig. 4: Nitrogen adsorption-desorption isotherm profile of SCBA-based mesoporous silica

3.4 Pore and Surface Characteristics

The mesoporous silica material was characterized using the BET method to determine pore characteristics such as pore diameter, pore volume, and specific surface area. The pore diameter provides insights into the type of pores present in the synthesized mesoporous silica. Table 3 displays the pore characteristics of the mesoporous silica produced using bagasse as the raw material. The analysis revealed that the specific surface area, pore volume, and pore radius of the synthesized SCBA-based mesoporous silica were 363.4 m2/g, 0.716 cc/g, and 1.5434 nm, respectively. These findings indicate that the resulting porous material falls within the category of mesoporous materials, given that its pore diameter ranges from 2-50 nm, precisely measuring 3.0868 nm. In comparison with the study conducted by Bae et al., 201031), the pore characteristics of the material synthesized from tetraethyl orthosilicate (TEOS) exhibited surface area, pore volume, and pore size of 422 m2/g, 1.02 cc/g, and 9.56 nm, respectively. The disparity in porosity can be attributed to the use of different silica sources and potential variations in the formation process of mesoporous silica32). Mesoporous silica derived from sugarcane bagasse exhibits a narrow distribution of pore radius with dominant pore size. The presence of numerous small dominant pores significantly contributes to the increased adsorption volume in mesoporous silica, as depicted in Fig. 5.

Table 3. Pore and surface characteristics of SCBA-based mesoporous obtained from N_2 adsorption measurement

Characteristics	Value
Surface area (m^2/g)	363.4
Pore radius (nm)	1.5434
Pore volume (cc/g)	0.716

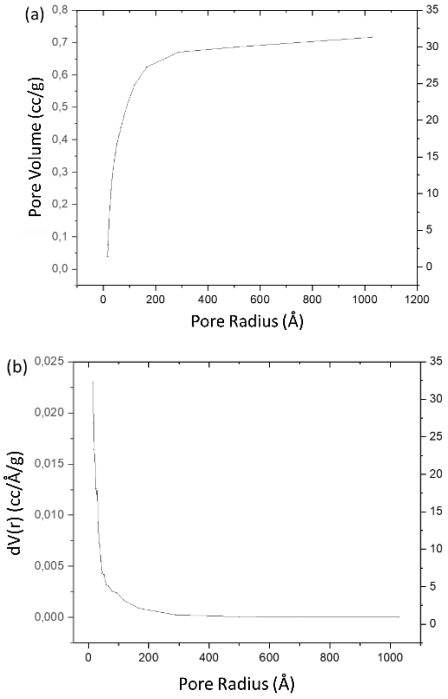

Fig. 5: Pore characteristic distribution of SCBA-based mesoporous silica: (a) Relation between pore size and pore volume; (b) BJH desorption

3.5 Identification of Crystal Structure

Figure 6 shows SAXS patterns of SCBA samples synthesized using Pluronic 123. The displayed graph has been rescaled to focus solely on the angle range of 1.0-2.5˚ in order to provide a clearer view of the peaks observed in the SAXS analysis. From the SAXS profiles, one intense peak identified at 2θ of 1.6° and two lower peaks identified at 2θ in the range of 1.65 to 3.0°. The obtained SAXS test results were then processed using the Bragg's Law equation to obtain the hkl planes of the main peak. The calculation diffraction angles of the mesoporous silica SAXS and the hkl planes can be found in Table 4. From the calculation, those three peaks represent the (110), (200), and (211) planes, respectively. These indices belong to the body-centered cubic (BCC) crystal structure with Im3m symmetry. In Fig. 7, presents

the result of TEM testing, revealing the ordered crystal structure of the resulting mesoporous silica material. The findings from the TEM testing corroborate the SAXS results, confirming that the crystal structure of the mesoporous silica material derived from SCBA is indeed BCC.

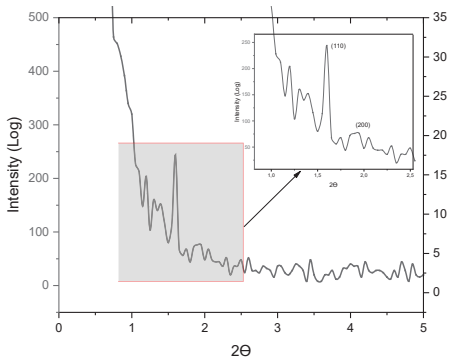

Fig. 6: SAXS pattern of SCBA-based mesoporous silica

Table 4. Calculation of diffraction angles from SAXS results of SCBA-based mesoporous silica

2θ	$2\text{Sin}\theta$	Ratio	M	hkl	d (nm)
1.6	0.0279	1.62	2	(110)	5.52
2.5	0.0436	3.93	4	(200)	3.53
3	0.0524	5.67	6	(211)	2.94

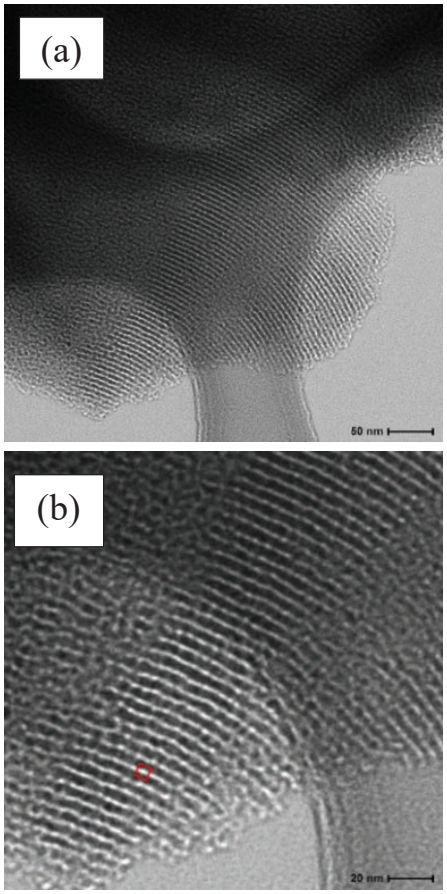

Fig. 7: TEM images for SCBA-based mesoporous silica: (a) 20 nm; (b) 50 nm magnification

3.6 Adsorption of Brilliant Green

The mesoporous silica was subjected to adsorption testing using a brilliant green solution for a duration of 4 hours. The initial concentration of the solution was 10 ppm. Samples of the adsorbed brilliant green dye solution were taken hourly and compared to the blanco solution. The time dependence of brilliant green dye adsorption on the SCBA-based mesoporous silica samples is shown in Fig. 8(b). The adsorption spectra and color changes from dark to pale green indicate an increase in pollutant uptake with prolonged contact time. The corresponding BG removal efficiency and adsorbate quantity can be seen in Fig. 8(a). Red visible light was present in the blanco solution as evidenced by the strongest peak, which appeared at a wavenumber of 625 nm and an absorption intensity of 5.85 A[33]. As the concentration of the brilliant green solution increases, the red spectrum reflects the green color. It can be observed that the absorbance intensity of the brilliant green solution decreases when adsorbed by the mesoporous silica. As the adsorption duration increases, the absorbance intensity at the maximum wavenumber decreases more noticeably. By using Equations (5) and (6), the adsorption capacity (qt) of mesoporous silica and the removal percentage of brilliant green dye (% removal) per hour can be obtained by referring to the graph of the test results. Here, the absorbance intensities of the blanco solution and the dye solution adsorbed at a specific time are represented by A_o and A_t, whereas the concentrations of the blanco solution and the dye solution adsorbed at a specific time are represented by C_t and C_o. V is the volume, m is the mass of the adsorbent (g), and qt is the absorption capacity at time t (mg/g)[34]. The uptake capacity and removal percentage of brilliant green for each hour are presented in Table 5. Based on Table 5, it can be inferred that the synthesized mesoporous silica is effective enough to adsorb the brilliant green dye contained in the solution. This is demonstrated by a removal percentage that is more than 50% after four hours. Via interactions between the adsorbent and adsorbate, the brilliant green adsorption mechanism involves the migration of the dye solution to the surface of the mesoporous silica. Brilliant green, which categorized as a cationic dye, electrostatically interacts with the negatively charged mesoporous silica at neutral pH[35]. In Fig. 8(b), it can be observed that after 4 hours of adsorption by mesoporous silica, the solution becomes nearly colorless. SCBA exhibits a favorable adsorption capacity and removal efficiency. However, it is important to note that the adsorption capability of SCBA remains lower compared to commercially available silica beads, possibly due to pore clogging caused by impurities originating from the silica source. Nevertheless, considering the intricate and costly production process of silica beads, SCBA shows promise as an alternative material for wastewater purification applications. To achieve even higher %removal, adsorption can be extended beyond 4 hours, allowing for a %removal

exceeding 50%.

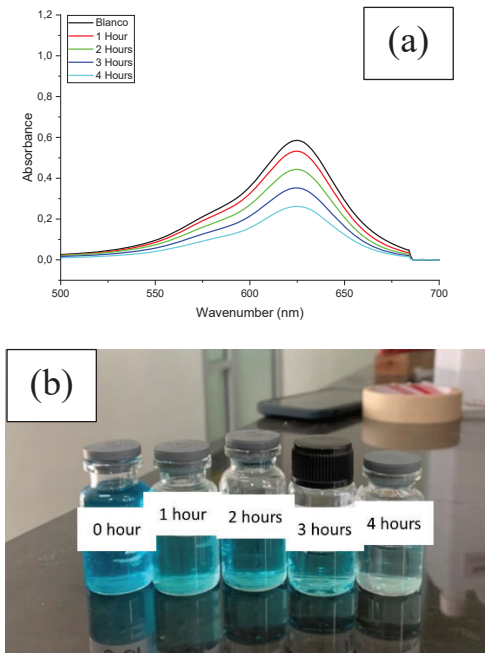

Fig. 8: (a) Absorption spectra of SCBA-based mesoporous silica; (b) Aqueous brilliant green dye solution with various adsorption time

Table 5. The uptake capacity and % Removal of SCBA-based mesoporous silica at each adsorption time

Adsorption Time (h)	Uptake Capacity (mg/g)	% Removal
1	0.91	9.1
2	2.42	24.2
3	3.98	39.8
4	5.51	55.1

4. Conclusion

The mesoporous silica derived from sugarcane bagasse ash as the silica source was successfully synthesized using Pluronic 123 surfactant as the directing agent. The resultant substance had an Im3m symmetric two-dimensional body-centered cubic (BCC) crystal structure. Because of the surfactants utilized during synthesis, the SCBA-based mesoporous silica's surface appearance was characterized by coarse aggregates with occasional spherical particles. The synthesized SCBA-based mesoporous silica possessed high surface area, pore radius, and pore volume, with values of 363.4 m^2/g, 1.5434 nm, and 0.716 cc/g, respectively. The H3 type isotherm profile indicated wedge-shaped pores with narrow distribution and dominant pores. FTIR analysis confirmed the presence of O-H, H-OH, and Si-O-Si functional groups indicating the successful sol-gel process. The synthesis of mesoporous silica exhibited three Si-O-Si groups, further validating the successful synthesis. In terms of adsorption capabilities, the SCBA-based mesoporous silica demonstrated a middle efficiency in removing brilliant green, with uptake capacity and removal percentage of 5.51 mg/g and 55.1% after a 4-hour adsorption time, respectively. Overall, the synthesized SCBA-based mesoporous silica showed promising characteristics and showed potential for applications in dye adsorption and other related fields.

Acknowledgements

The work was supported by a research grant from the Indonesian Ministry of Education, Culture, Research, and Technology for the "Penelitian Kompetitif Nasional Program 2024" (Grant No. NKB-1143/UN2.RST/HKP.05.00/2023). The authors would also like to thank the Advanced Materials Laboratory Department of Metallurgical and Materials Engineering, Faculty of Engineering, Universitas Indonesia.

References

1) R.P. Putra, M.R.R. Ranomahera, M.S. Rizaludin, R. Supriyanto, and V.A.K. Dewi, "Short communication: investigating environmental impacts of long-term monoculture of sugarcane farming in indonesia through DPSIR framework," Biodiversitas, 21 (10) 4945–4958 (2020). doi:10.13057/BIODIV/D211061.
2) A.E. Souza, S.R. Teixeira, G.T.A. Santos, F.B. Costa, and E. Longo, "Reuse of sugarcane bagasse ash (SCBA) to produce ceramic materials," Journal of Environtal Management, 92 (10) 2774–2780 (2011). doi: 10.1016/j.jenvman.2011.06.020.
3) R.K. Ahmad, S.A. Sulaiman, M. Amin, B.A. Majid, S. Yusuf, S.S. Dol, and H.A. Umar, "Assessing the technical and environmental potential of coconut shell biomass: experimental study through pyrolysis and gasification," EVERGREEN Joint Journal of Novel Carbon Resource Sciences & Green Asia Strategy, 10 (1) 585–593 (2023). https://doi.org/10.5109/6782165
4) Z.F. Zahara, "Economic assessment of the sugarcane-based bio-refinery in indonesia," Evergreen, 5 (2) 67–77 (2018). doi:10.5109/1936219.
5) A.J. Khan, J. Song, K. Ahmed, A. Rahim, P.L. Onófrio Volpe, and F. Rehman, "Mesoporous silica MCM-41, SBA-15 and derived bridged polysilsesquioxane SBA-PMDA for the selective removal of textile reactive dyes from wastewater," Journal of Molecular Liquids, 298 (2020). doi:10.1016/j.molliq.2019.111957.
6) F. Tang, L. Li, and D. Chen, "Mesoporous silica nanoparticles: synthesis, biocompatibility and drug delivery," Advanced Materials, 24 (12) 1504–1534 (2012). doi:10.1002/ADMA.201104763.
7) M. Sari Yilmaz, "Graphene oxide/hollow mesoporous silica composite for selective adsorption of methylene blue," Microporous and Mesoporous Materials, 330 (2022). doi:10.1016/j.micromeso.2021.111570.
8) W.K. Cheah, Y.L. Sim, and F.Y. Yeoh, "Amine-

functionalized mesoporous silica for urea adsorption," Materials Chemistry and Physics, 175 (2016). doi:10.1016/j.matchemphys.2016.03.007.
9) S.H. Wu, and H.P. Lin, "Synthesis of mesoporous silica nanoparticles," Chemical Society Reviews, 42 (9) 3862–3875 (2013). doi:10.1039/C3CS35405A.
10) V. Fathi Vavsari, G. Mohammadi Ziarani, and A. Badiei, "The role of SBA-15 in drug delivery," RSC Advances, 5 (111) 91686–91707 (2015). doi:10.1039/C5RA17780D.
11) W.J.J. Stevens, K. Lebeau, M. Mertens, G. Van Tendeloo, P. Cool, and E.F. Vansant, "Investigation of the morphology of the mesoporous SBA-16 and SBA-15 materials," The Journal of Physical Chemistry B, 110 (18) 9183–9187 (2006). doi:10.1021/jp0548725.
12) H. Al Hijri, J.F. Fatriansyah, N. Sofyan, and D. Dhaneswara, "Potential use of corn cob waste as the base material of silica thin films for anti-reflective coatings," Evergreen, 9 (1) 102–108 (2022). doi:10.5109/4774221.
13) H. T. Thu, L. T. Dat, and V. A. Tuan, "Synthesis of mesoporous SiO2 from rice husk for removal of organic dyes in aqueous solution," Vietnam Journal of Chemistry, 57 (2) 175-181 (2019). doi: 10.1002/vjch.201900012.
14) D. Dhaneswara, H.S. Marito, J.F. Fatriansyah, N. Sofyan, D.R. Adhika, and I. Suhariadi, "Spherical SBA-16 particles synthesized from rice husk ash and corn cob ash for efficient organic dye adsorbent," Journal of Cleaner Production, 357 131974 (2022). doi:10.1016/J.JCLEPRO.2022.131974.
15) N. Pal, E.B. Cho, and D. Kim, "Synthesis of ordered mesoporous silica/ceria-silica composites and their high catalytic performance for solvent-free oxidation of benzyl alcohol at room temperature," RSC Advances, 4 (18) 9213–9222 (2014). doi:10.1039/c3ra47464j.
16) D. Navas, S. Fuentes, A. Castro-Alvarez, and E. Chavez-Angel, "Review on sol-gel synthesis of perovskite and oxide nanomaterials," Gels, 7 (4) (2021). doi:10.3390/gels7040275.
17) B. Deljoo, T. Jafari, R. Miao, M.-P. Nieh, S.L. Suib, and M. Aindow, "Surfactant selection as a strategy for tailoring the structure and properties of UCT manganese oxides," Materials & Design, 180 107902 (2019). doi: 10.1016/j.matdes.2019.107902.
18) A.S. Idris, S. Ghosh, H. Jiang, and K. Hamamoto, "A multi-layer stacked all sol-gel fabrication technique for vertical coupled waveguide," Evergreen, 4 (2–3) 12–17 (2017). doi:10.5109/1929657.
19) D. Bokov, A. Turki Jalil, S. Chupradit, W. Suksatan, M. Javed Ansari, I.H. Shewael, G.H. Valiev, and E. Kianfar, "Nanomaterial by sol-gel method: synthesis and application," Advances in Materials Science and Engineering, 2021 (2021). doi:10.1155/2021/5102014.
20) G.J. Owens, R.K. Singh, F. Foroutan, M. Alqaysi, C.M. Han, C. Mahapatra, H.W. Kim, and J.C. Knowles, "Sol-gel based materials for biomedical applications," Progress in Materials Science, 77 (2016). doi:10.1016/j.pmatsci.2015.12.001.
21) R. Scott, "Silica Gel and Bonded Phases: Their Production, Properties and Use in LC," 1st ed., Chichester, 1993.
22) E. Mohajeri, and G. Noudeh, "Effect of temperature on the critical micelle concentration and micellization thermodynamic of nonionic surfactants: polyoxyethylene sorbitan fatty acid esters," E-Journal of Chemistry, 9 (4) 2268–2274 (2012).
23) E. Petala, K. Dimos, A. Douvalis, T. Bakas, J. Tucek, R. Zbořil, and M.A. Karakassides, "Nanoscale zero-valent iron supported on mesoporous silica: characterization and reactivity for Cr(VI) removal from aqueous solution," Journal of Hazardous Materials, 261 (2013). doi:10.1016/j.jhazmat.2013.07.046.
24) B. Baumgartner, J. Hayden, J. Loizillon, S. Steinbacher, D. Grosso, and B. Lendl, "Pore size-dependent structure of confined water in mesoporous silica films from water adsorption/desorption using ATR–FTIR spectroscopy," Langmuir, 35 (37) 11986–11994 (2019). doi:10.1021/acs.langmuir.9b01435.
25) R. Rubaya, F. Afroze, S. Ahmed, M. Miran, and M. Abu, "Control of the porosity and morphology of ordered mesoporous silica by varying calcination conditions," Material Today:Proceedings, 15 546–554 (2019).
26) F. Nhavene, G. Ferreira, A. Id, J. Araujo, and D. Gomes, "Biodegradable polymers grafted onto multifunctional mesoporous silica nanoparticles for gene delivery," ChemEngineering, 2 (24) 1–16 (2018).
27) Y. Nakama, "Cosmetic science and technology: theoretical principles and applications," 231–244 (2017).
28) D. Dhaneswara, and N. Sofyan, "Effect of different pluronic P123 triblock copolymer surfactant concentrations on SBA-15 pore formation," International Journal of Technology, 7 (6) 1009–1015 (2016). doi:10.14716/ijtech.v7i6.3412.
29) F. Ambroz, T. Macdonald, V. Martis, and I. Parkin, "Evaluation of the BET theory for the characterization of meso and microporous MOFs," Small Methods, 2 (11) 1–17 (2018).
30) L. Xu, J. Zhang, J. Ding, T. Liu, G. Shi, X. Li, W. Dang, Y. Cheng, and R. Guo, "Pore structure and fractal characteristics of different shale lithofacies in the dalong formation in the western area of the lower yangtze platform," Minerals, 10 (1) 72 (2020). doi: 10.3390/min10010072.
31) A. Grosman, and C. Ortega, "Nature of capillary condensation and evaporation processes in ordered

porous materials," Langmuir, 21 (23) 10515–10521 (2005). doi:10.1021/la051030o.
32) J. Bae, S. Hwang, K. Song, J. Jeon, Y. Ko, and J. Yim, "Synthesis of functionalized mesoporous material with various organo-silanes," Journal of Nanoscience and Nanotechnology, 10 (1) 189–195 (2010).
33) D. Dhaneswara, J. F. Fatriansyah, F. W. Situmorang, and A. N. Haqoh, "Synthesis of amorphous silica from rice husk ash: comparing HCl and CH3COOH acidification methods and various alkaline concentrations," International Journal of Technology, 11 (1) 200–208 (2020). doi: 10.14716/ijtech.v11i1.3335.
34) D. Dhaneswara, N. Zulfikar, J.F. Fatriansyah, M.S. Mastuli, and I. Suhariadi, "Adsorption capacity of mesoporous SBA-15 particles synthesized from corncobs and rice husk at different ctab/p123 ratios and their application for dyes adsorbent," Evergreen, 10 (2) 924–930 (2023). doi:10.5109/6792887.
35) K. Selvan, K. Swaminathan, and K. Chae, "Decolourization of azo dyes and a dye industry effluent by a white rot fungus thelephora sp," Bioresource Technology, 88 (2) 115–119 (2003).